Journal of Education and Science (ISSN 1812-125X)

Measurement of Reduced Electromagnetic Transition (BM1/BE2) in the Strongly Coupled Bands in 161Er Nuclei

J. L. Mawlan [1*], M. I. Mohammed [2]

[1] Department of Physics, Faculty of Science and Health, Koya University, Koya 44023, Kurdistan Region – F.R. Iraq
[2] Department of Physics, College of Science, University of Raparin, Rania, Sulaymaniyah, 46012, Iraq

Article information

Article history:
Received: November 05, 2025
Revised: December 25, 2025
Accepted: January 06, 2026
Available online: April 01, 2026

Keywords:
B(M1)/B(E2) Ratios
^{161}Er Nuclei
Quasiparticle Configuration

Correspondence:
Jutyar Luqman Mawlan
jutyar.luqman@uor.edu.krd

Abstract

In this study, we examined the ratios of reduced electromagnetic transition probabilities for strongly coupled bands in ^{161}Er nuclei using the Gammasphere spectrometer. The nuclei were populated via the ^{116}Cd (^{48}Ca, 3γ) fusion-evaporation reaction at a beam energy of 215 MeV. Experimental B(M1)/B(E2) ratios were extracted from the coincidence spectra using the Radware software suite. These results were compared with theoretical calculations to investigate the evolution of magnetic dipole and electric quadrupole transition strengths within the coupled bands. The observed B(M1)/B(E2) ratios are consistent with systematic trends in neighbouring isotopes; however, they exhibit a reduced M1 strength, particularly at low spin, as the nucleon number increases. The observed decrease indicates a reduction in the magnetic dipole component associated with changes in the underlying quasiparticle configuration. The experimental results closely match theoretical predictions, thereby validating the proposed configurations and expanding the systematics of B(M1)/B(E2) ratios within the Er isotopic chain.

DOI: 10.33899/jes.v35i2.53767,

1. Introduction

Various models have been used to explain the distribution of protons and neutrons in the nucleus and to correlate this distribution with its properties, such as binding energies, deformation, and rotation. For instance, the liquid-drop model [1], which conceptualises the nucleus as a charged liquid drop, addresses bulk properties such as fission, binding energies, and collective oscillations. Nevertheless, this model could not explain the existence of so-called “magic numbers” and the stability of some nuclei. To overcome this, the nuclear shell model [2]. It was developed with quantised single-particle energies in an average potential well. The model explained the magic numbers by including spin–orbit coupling and provided a microscopic account of nuclear structure by describing how nucleons fill individual shells in accordance with the Pauli principle. Later, for deformed nuclei, the Nilsson model. Extended the shell model by incorporating quadrupole deformation in the potential. This modification allowed spherical shells to be divided into Nilsson orbitals, a foundation on which to describe rotational bands and quasiparticle excitations in well-deformed nuclei. Together, the models offer complementary pictures: the liquid-drop model accounts for collective bulk motion, the shell model accounts for single-particle arrangements, and the Nilsson model reconciles the two by accounting for how nucleons occupy orbitals in deformed systems. A process fusion evaporation reaction that produces a heavy ion. A highly excited compound nucleus is created when an ion projectile collides with a target nucleus. This nucleus then cools by releasing light particles like protons, neutrons, or α particles. The residual nucleus generated depends on the selection of the evaporation channel. At a beam energy of 215 MeV, the reaction ^{116}Cd (^{48}Ca, 3γ) was used to populate the isotope **^{161}Er**. Three neutrons (xn=3) were emitted from the excited compound nucleus, forming **^{161}Er**.

This reaction pathway provides an effective method for producing the odd-A erbium isotope ^{161}Er for detailed spectroscopic investigation. A high-efficiency γ-ray detector array (Gammasphere), which enables accurate coincidence spectroscopy and level scheme construction, was used to quantify γ-ray emissions during de-excitation and to investigate their rotational structures [3]. The standard RADWARE program package [7] was used to analyse the γ-ray spectra obtained with Gammasphere. This allowed for the creation of level schemes for the erbium isotopes, background suppression, and coincidence gating. These spectra are used experimentally to investigate rotational alignments, quasiparticle excitations, and lowered transition probability ratios in these nuclei.

Previous studies have systematically investigated the reduced electromagnetic transition probability ratios B(M1)/B(E2) for erbium isotopes, revealing clear differences between the strongly coupled multi-quasiparticle (C1) and single-quasiparticle (C2) rotational bands[1, 4]. However, the heaviest odd-mass isotope in this chain, **^{161}Er**, has not been explored within this framework, leaving a gap in understanding how the magnetic dipole (M1) strength and quasiparticle–rotor coupling evolve with increasing neutron number. The present work, therefore, aims to extend these investigations to **^{161}Er**, to test the theoretically predicted systematic reduction of M1 strength with neutron number [5], and to determine the B(M1)/B(E2) ratios for this nucleus experimentally for the first time.

Ultimately, the current study of rotational structures in ^{161}Er contributes to the systematics of B(M1)/B(E2) ratios along the erbium isotope chain and provides new evidence for the microscopic origin of backbending. More significantly, the observed decline in M1 strength as the neutron number rises emphasises how pairing correlations and shell filling control quasiparticle–rotor coupling.

2. The experimental data

The experimental data summarized here correspond to measurements previously carried out at the ATLAS facility at Argonne National Laboratory. The experiment involved fusion–evaporation reactions in which excited states of several nuclei, including ^{161}Er, were populated using a ^{48}Ca beam incident at 215 MeV on enriched (98.7%) ^{116}Cd targets. **In the original experiment**, two self-supporting ^{116}Cd foils with a total thickness of 1.3 mg/cm2 were used. γ rays emitted from the reaction products were detected using the Gammasphere spectrometer. Approximately 1.9×10^9 events were recorded through rapid coincidence firing of at least seven of the 110 Compton-suppressed HPGe detectors. Over a five-day period, about 1.4 × 1011triple and 3.5 × 1010 quadruple coincidence events were accumulated. The data were processed into four-dimensional (E_γ^4) hypercubes and three-dimensional (E_γ^3) cubes following the procedures described in Ref [6]. **For the present work**, only the γ-ray coincidence data for **^{161}Er** were analyzed. One-dimensional spectra were extracted, and gates were placed on stretched quadrupole (E2) transitions. Based on the predetermined angular configuration of the Gammasphere rings, the data were divided accordingly for further analysis.

3. Level scheme of yrast bands of 156-161 Er nuclei.

Figure 1 presents the partial level scheme of the yrast bands for the $^{156\text{-}161}$ Er nuclei, which is constructed from gamma-ray analysis data using Radware data analysis software. It depicts the nuclear energy levels, spin, parity, and gamma-ray transitions between the level energies of the rotational band of each isotope, noting that the energy levels are accompanied by their respective spin and parity assignments based on prior experimental works using the quasiparticle and rotational configuration schemes. [7, 8].

Nuclear energy levels in the yrast bands of even-even (even-A) ^{156,158,160}Er nuclei exhibit prominent features of well-deformed rotational bands. Their yrast bands start with 0^+ spin and parity, based on the vacuum state 0- quasiparticle configuration and follow the expected $(E \propto I(I+1))$ relation for a rotational spectrum. The spacing between the nuclear energy levels provides evidence of a strongly collective rotation, which is consistent with a deformed prolate nuclear shape. The increasing moment of inertia with rotational frequency indicates the gradual alignment of high-j Nilsson orbitals, likely due to the gradual breaking of nucleon pairs experiences backbending [7, 8]. The odd-A ^{157,159,161}Er nuclei have an unpaired neutron, forming yrast sequences correspond to 1-quasiparticle configurations on Nilsson orbitals close to the Fermi surface (e.g., $\nu 7/2^-[514], \nu 9/2^+[624]$) [9, 10]. For these configurations, the band heads are relatively low (e.g, ~267 keV for ^{161}Er) and are followed by an increase in spin. These bands show lower collectivity than in the even-even nuclei, which is evidenced by the irregular spacing of the levels and some hinge-like signature splitting.

The structural evolution of several isotopes as the neutron number rises can be directly compared thanks to this compilation. For example, although ^{156,158,160}Er display very regular revolving bands, the odd-A isotopes show more complex behaviours due to the interaction between degrees of freedom for single particles and collective particles. The excitation energy consistently shifts upward with neutron number, especially in even-even isotopes, reflecting changes in pairing correlations and deformation. [11].

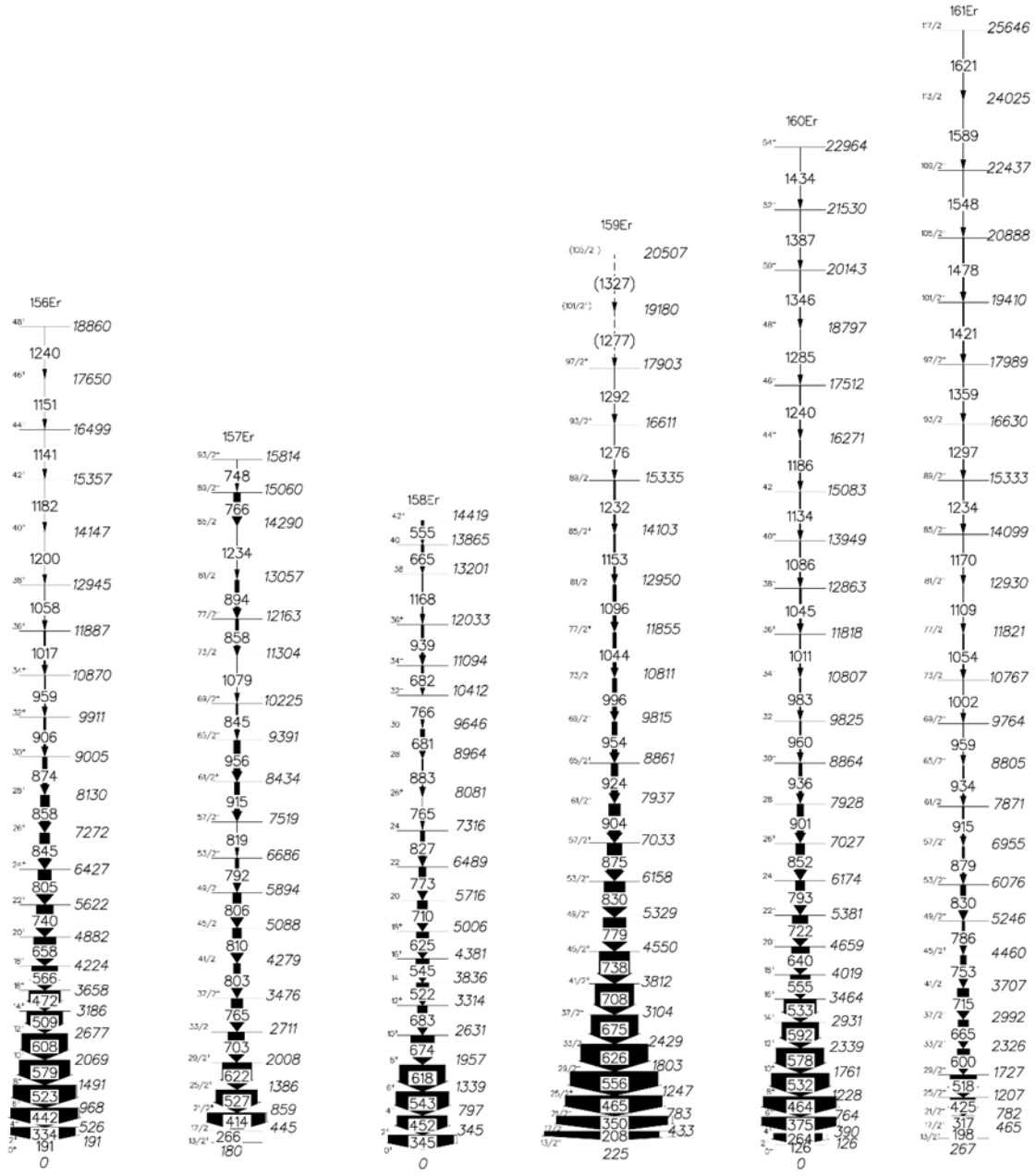

Figure 1. Partial level Scheme of yrast bands of $^{156\text{-}161}$Er nuclei.

3.1 Alignment and rotational properties of Band

Alignment (aligned angular momentum) as a function of rotational frequency plots [12]can be used to experimentally identify the majority of nuclear structure features of rotational bands. These properties can be derived from the spin of the energy level and gamma transition energies. The reference angular momentum is subtracted to provide this alignment.

$$i_x(\omega) = I_x(\omega) - I_{x,ref}(\omega) \quad (1)$$

$$e_{ex}(\omega) = E(\omega) - E_{ref}(\omega) \quad (2)$$

I_x is the aligned spin $I_x = \sqrt{I(I+1) - K^2}$ at a given spin, the rotational frequency is related to the gamma-ray transition energy $\omega = E_\gamma / \Delta I_x \approx E_\gamma / 2\hbar$, whereas the rotational reference $I_{x,ref}(\omega)$ and $E_{ref}(\omega)$ are given by

$$I_{x,ref}(\omega) = (J_\circ + J_1)\omega - i_\circ \quad (3)$$

$$E_{ref}(\omega) = \frac{-1}{2}\omega^2 J_\circ \frac{-1}{4}\omega^4 J_1 + \frac{1}{8}J_\circ^{-1} \quad (4)$$

In order to guarantee that the alignment for the yrast band of $^{156\text{-}161}$Er at low rotational frequencies is roughly zero, Harries' parameters [13] J_0 =27.8.0MeV^{-1} and J_1 =45.0MeV^{-3} were selected from the mean values for two even-even neighbours with an offset i_0=0. Following the initial backbend, these values give the quasineutron configuration consistent alignment. Figures 2 and 3 display the alignment pattern for the yrast band of $^{156\text{-}161}$Er nuclei.

3.2 Alignment Comparison of odd-A and even-A neighbouring Er isotopes:

The yrast bands in all Erbium nuclei from $^{156\text{-}161}$Er exhibit a first backbending, which arises due to the Coriolis force breaking the first or second pair of $i_{13/2}$ quasineutrons (denoted as pairs AB for even-N isotopes and BC for odd-N isotopes), followed by a second backbending due to the alignment of a pair of $h_{11/2}$ quasiprotons A_pB_p , as illustrated in Figures 2 and 3. In the present work, the experimental alignments were calculated using the reference parameters (J_0, J_1) adopted from the previous section. These calculations were performed for the yrast band in ^{161}Er, and compared with the yrast bands of odd-A neighbouring Erbium isotopes possessing signature and parity $(\alpha, \pi) = (+, +\frac{1}{2})$. The configuration of the yrast bands in ^{157}Er and ^{161}Er is based on the [6 5 1]3/2 $i_{13/2}$ orbital, while for ^{161}Er. The configuration is based on the [6 4 2]5/2 i13/2 odd nucleon subshell. The alignment of the angular momentum as a function of the rotational frequency in the yrast bands of the odd Erbium isotopes ^{157}Er[14] [15] [16]^{169}Er, and ^{161}Er [17] has been systematically compared. The yrast bands with signature and parity (+, +1/2) in these odd-A isotopes are associated with one quasineutron configuration. They start with the alignment angular momentum of approximately 1ħ. At low rotational frequencies, the yrast band exhibits collective rotational motion that corresponds to prolate nuclear shapes.

Figure 2 displays the experimental alignment plots up to the termination states for the yrast bands with signature and parity (+,1/2) in the odd-N isotopes $^{157, 159, 161}$Er. Consistent with its collective features, the yrast band in ^{161}Er exhibits a band crossing with a gain in alignment of 6.87ħ at a rotational frequency of 0.38 MeV/ħ. Alignment gains of 9.43ħ and 6.34ħ, respectively, alter the collective behaviour in the $^{157\text{-}161}$Er yrast bands. The second pair of $i_{13/2}$ quasineutron (BC) aligns with these gains at crossing frequencies of 0.394 MeV/ħ and 0.353 MeV/ħ, respectively. Because of the presence of (A) quasineutron configuration in all yrast bands, AB quasinutron crossings in odd-N $^{157\text{-}161}$Er isotopes are Pauli blocked, as shown in Figure 2. As a result, they exhibit BC band crossing to align the same pair of $i_{13/2}$ quasineutrons BC at a rotational frequency, as shown in Table 1. Following BC crossing, the bands' behaviour shifts from collective-prolate to non-collective weakly deformed oblate mode up to their termination states [18] due to the abnormalities that arise from breaking a pair of $h_{11/2}$ quasiprotons A_pB_p. The yrast band (+, 1/2) in nuclei $^{157, 159, 161}$Er obtains an ABC A_pB_p configuration at the same rotational frequency (0.46 MeV/ħ) with a gain in alignment of ≈ approximately 4-6. This behaviour was caused by the compensation between the increase in gain due to the alignment of BC quasi neutrons and the decrease in the neutron pair gap. This interpretation confirms that the yrast band in those nuclei has the same amount of mixing between the proton Fermi surface and highly alignable low Ω components of the $h_{11/2}$ protons, which does not change as the nuclei rotate.

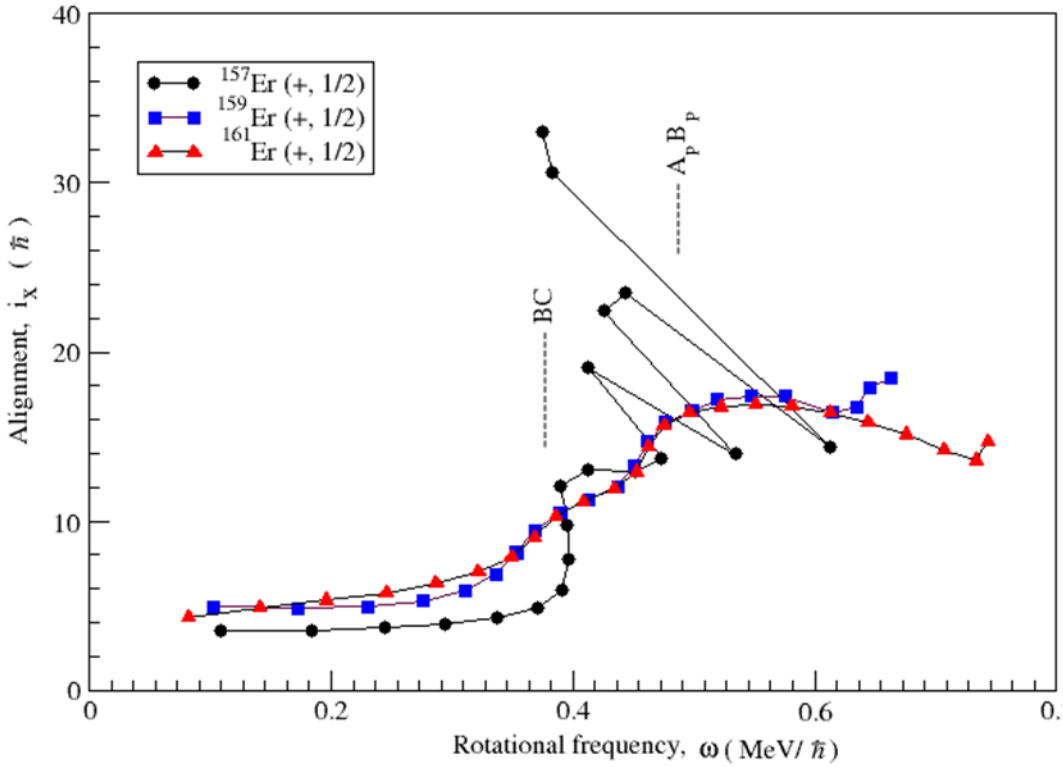

Figure 2. Experimental alignment versus rotational frequency of yrast bands of $^{157, 159, 161}$Er, The Harris reference parameters are chosen to be J_0=27.8MeV^{-1} and J_1=45.0MeV^{-3}

Figure 3 reveals systematic changes in AB neutron crossing and A_pB_p proton pairs. AB crossing frequency decreases with increasing neutron number, for even-N ($^{156, 158,160}$Er) nuclei at rotational frequencies of $\hbar\omega$=0.304,0.289, and 0.282 MeV, resulting in gains in alignment of 10.81, 9.66, and 9.62 $\hbar$, respectively. In ^{156}Er, the band exhibits a pronounced backbend at a rotational frequency of $\hbar\omega$ = 0.304 MeV/$\hbar$. Beyond this point, the band carries an aligned angular momentum of approximately 10.81$\hbar$ at rotational frequencies greater than 4 MeV/$\hbar$, up to the terminating state 42$^+$. Sudden structural changes observed at high spins provide evidence of a transition in the nuclear configuration mode, indicating a loss of collective motion and the development of a non-collective oblate nuclear shape. The decrease in the AB crossing is related to the reduction of neutron pair correlations [19], as well as gain in alignment decrease with neutron number for ($^{156-, 158, 160}$Er) occurs as a result of the increase in pairing energy gap and spreading between the Fermi level and highly alignable low Ω $i_{13/2}$ neutron components, which lead to the increase of quadrupole deformation.

The dominant $h_{11/2}$ proton band crossing (A_pB_p) occurs at rotational frequencies that increase with the neutron number, for both even-A and odd-A Er nuclei. This crossing takes place within the rotational frequency range 0.4≤ ω ≤ 0.47 MeV/ħ. In addition, the alignment of the $h_{11/2}$ Quasiprotons increases with increasing neutron number. The observed shift in both the crossing frequency and the alignment of the A_pB_p quasiprotons can be explained by changes in nuclear quadrupole deformation with neutron number, as interpreted by Riley (1984) and Simpson et al. (1987). According to the Nilsson model, the proton Fermi surface lies close to the Ω=7/2 component of the $h_{11/2}$ proton subshell. The degree of proton alignment depends on the amount of mixing between the Ω=7/2 level and the low-Ω components $h_{11/2}$, resulting from the increase in quadrupole deformation with neutron number, which is influenced by nuclear rotation. This deformation causes the Ω=7/2 and Ω=1/2 levels to move further apart, thereby reducing their mixing.

After (ApBp) proton crossing, the yrast band in $^{158, 160}$Er presents an anomaly observation due to a strong up bend at rotational frequencies 0.585 and 0.673 MeV/ħ, respectively, known as unpaired band crossing[20, 21], which is attributed to the exchange of a pair of neutrons in levels of the different signature partner bands for both signature partner parity bands at high rotational frequencies, and couple both pairs to the signature and parity $(\alpha, \pi) = (+,0)$. The quantitative changes in alignment and crossing frequencies in even-A $^{156, 158,160}$Er nuclei are shown in Table 2. The quasiparticle configurations of the yrast band in $^{156-161}$Er nuclei [24, 25] are listed in Table 3.

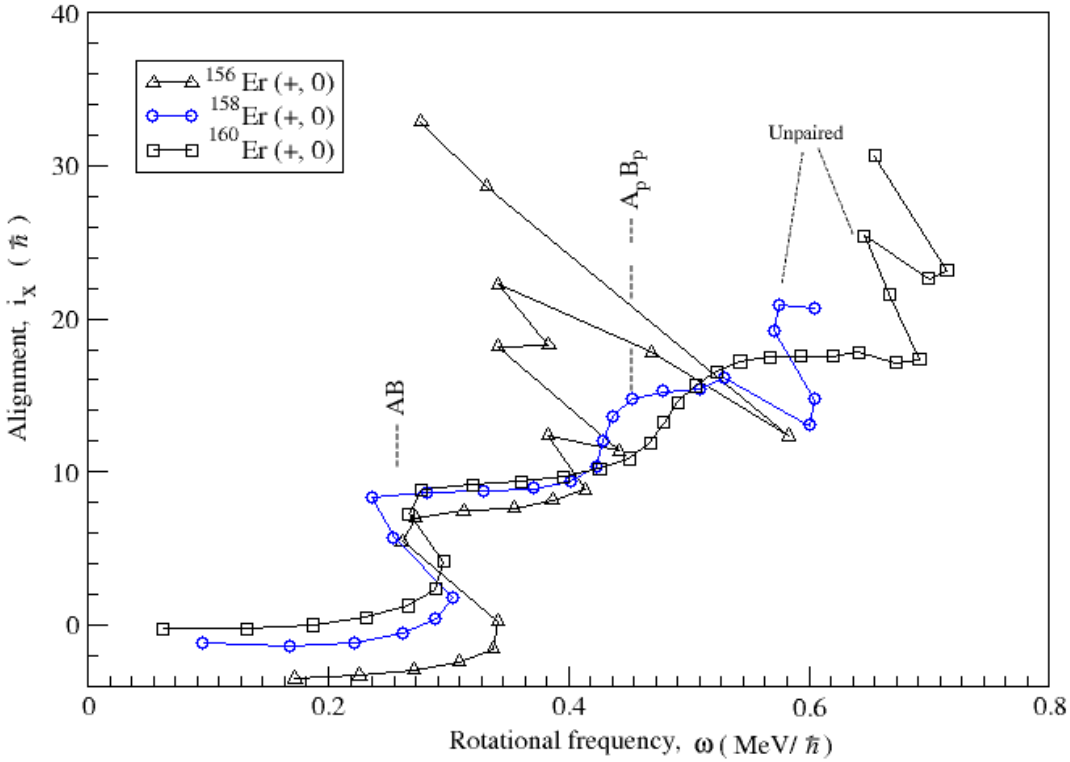

Figure 3. Experimental alignment versus rotational frequency yrast bands of $^{156, 158, 160}$Er, The Harris reference parameters are chosen to be J_0 =27.8.0MeV^{-1} and J_1 =45.0MeV^{-3}

Table 1. Explains crossing rotational frequencies and alignment gains for BC neutron and A_pB_p proton band crossings in odd-N $^{157, 159, 161}$Er nuclei

Isotopes	Start i_x ħ	BC ω_c	$\Delta i_{x(1)}$ ħ	A_pB_p ω_c	$\Delta i_{x(2)}$ ħ
^{157}Er (+, 1/2)	3.52	0.394	9.43	0.46	6.00
^{159}Er (+, 1/2)	3.60	0.360	6.34	0.46	6.06
^{161}Er (+, 1/2)	4.25	0.370	4.3	0.47	4

Table 2. Explains rotational crossing frequencies and alignment gains for AB neutrons and A_pB_p proton pairs, and unpaired band crossings in even-N nuclei.

Isotopes	AB	Δi_{x1} (ħ)	A_pB_p	Δi_{x2} (ħ)	Unpaired	Δi_{x3} (ħ)
^{156}Er	0.304	10.81	0.402	3.5	–	–
^{158}Er	0.289	9.66	0.429	6.47	0.585	5.68
^{160}Er	0.282	9.62	0.470	8.01	0.673	7.87

Table 3. Explains the quasiparticle configurations of the yrast band in $^{156\text{-}161}$Er nuclei [24, 25].

Yrast band	Configuration
^{157}Er	A→ ABC
^{158}Er	0 → BCAD → BCAD → A_pB_p
^{159}Er	A → ABC → ABC⊗A_pB_p
^{160}Er	0 → AB → AB⊗A_pB_p *and EF and, or CD*
^{161}Er	[642]5/2$^+$→[642]5/2$^+$ BC→[642]5/2$^+$ BC⊗A_pB_p

4. Ratio of Reduced Transition Probabilities BM1/BE2 for Strongly Coupled bands C1 and C2 ^{161}Er

The lowered transition probabilities, which are commonly stated as the ratio B(M1)/B(E2) for stretched M1 and E2 transitions, aid in the verification of a suggested nuclear structure. Donau and Frauendorf's semi-classical method can be used to hypothetically determine these ratios.

$$\frac{B(M1:I\rightarrow I-1)}{B(E2:I\rightarrow I-2)} = \frac{12}{fQ_0^2 COS^2(\gamma+30^\circ}\left[1-\frac{K^2}{(I-\frac{1}{2})^2}\right]^{-2}\{\left(1-\frac{K^2}{I^2}\right)^{\frac{1}{2}}[K_1(g_1-g_R)\left(1\pm\ \frac{\Delta e'}{\omega}\right)+\sum_n K_n(g_n-g_R)]-\ \frac{K}{I}[(g_1-g_R)i_1+\sum_n(g_n-g_R)i_n]\}^2 \quad (5)$$

Where K_1, g_1 i_1 stand for the K value, g-factor, and alignment of the quasiparticle that causes the signature splitting in a configuration, and Q_0 is the quadrupole moment. The state's shell configuration affects the single-particle g-factor's value. The rotating g-factor, which is commonly assumed to be Z/A, is denoted by g_R, whereas K=nKn denotes the entire K value.

It is possible to evaluate the reduced B(M1)/B(E2) transition probability ratios when both ΔI = 1 and 2 transitions are permitted in the decay out of an excited nuclear state. The measured γ-ray energy and efficiency-corrected intensities were used to experimentally compute the B(M1)/B(E2) ratios using the standard relation.

$$\frac{B(M1;I\rightarrow I-1)}{B(E2;I\rightarrow I-2)} = 0.697\ \frac{\left(E_\gamma(I\rightarrow I-2)\right)^5}{(E_\gamma(I\rightarrow I-1))^3}\times\frac{1}{\lambda}\frac{1}{\lambda(1+\delta^2)}\left[\frac{\mu_N^2}{e^2b^2}\right] \quad (6)$$

Where,

$$\lambda = I_\gamma(I\rightarrow I-2)/I_\gamma(I\rightarrow I-1) \quad (7)$$

Where E_γ is measured in MeV and I_γ and E_γ are the γ-ray energy and intensities, respectively. Spectra generated by gating above the level of interest were used to obtain the experimental ratios.

4.1 Level Scheme and γ-ray Coincidence Spectra of the Strongly Coupled Bands in ^{161}Er.

Figure 4 illustrates the energy-level diagram of the strongly coupled bands C1 and C2 in ^{161}Er determined in the present work. Band C1 is built on the lowest spin state I=5/2$^-$ and extends up to the highest observed spin I=95/2$^-$. The maximum linking transition, corresponding to ΔI = 1, occurs at spin I=29/2$^-$. Band C2 is built on the lowest spin I=11/2$^-$ and extends up to I=35/2$^-$, with the strongest linking transition observed at the top of the band (I=35/2$^-$). The detailed configuration assignments for both bands are provided in Table 4. In general, the transition energies in C2 are higher than those observed in C1.

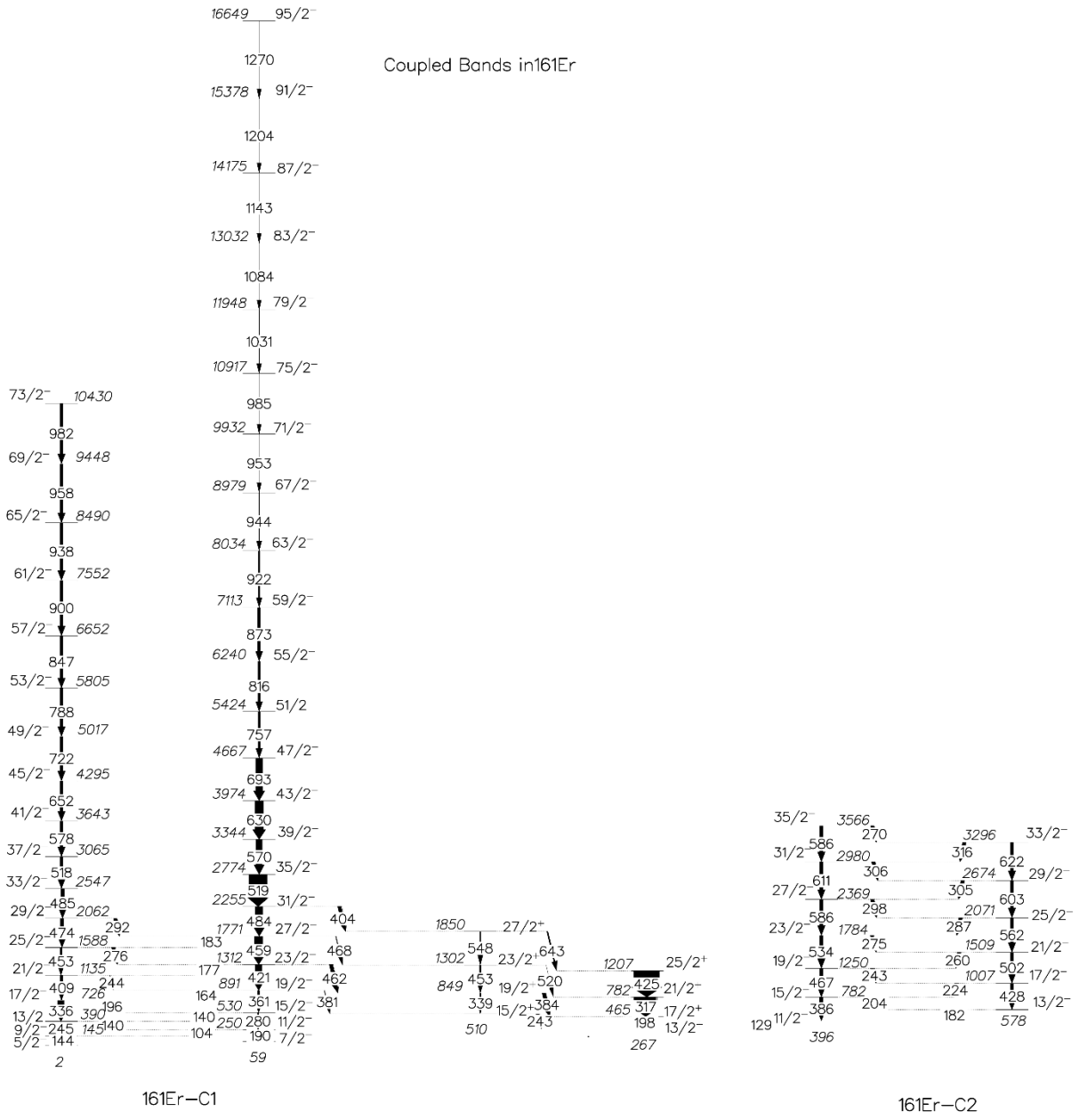

Figure 4. Partial level scheme of ^{161}Er, showing the strongly coupled bands C1 and C2 constructed in the present work. This figure also presents the yrast band γ–ray spectrum of ^{161}Er, measured using the RADWARE analysis program with a triple-gate sum over 198-879 keV transitions. Strong peaks at 198, 317, 425, and 518keV follow the core of the rotational cascade, while the decaying band is also observed to high-spin at higher-γ energies up to 1478 keV [26]. Figure 5 is the γ-ray spectrum of the strongly coupled band in ^{161}Er C1 obtained using the Radware program with a triple coincidence gate on the 421, 459, and 484-keV transitions [26]. Figure 6 is the γ-ray spectrum of the strongly coupled band in ^{161}Er C2 obtained with a triple coincidence gate on the 204- and 242-keV transitions [26, 27].

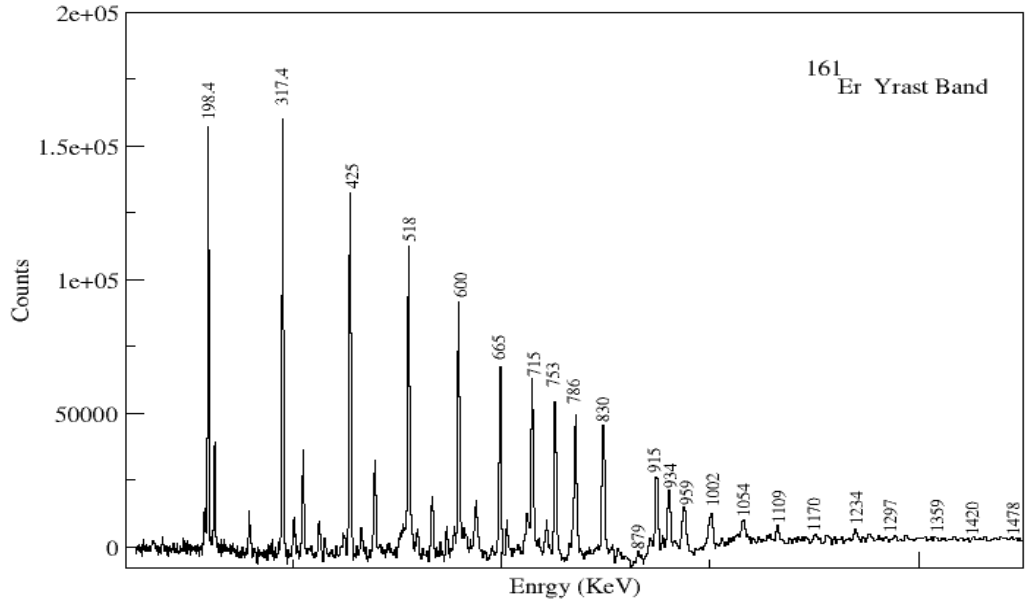

Figure 4. γ-ray coincidence spectrum for the yrast band in ^{161}Er

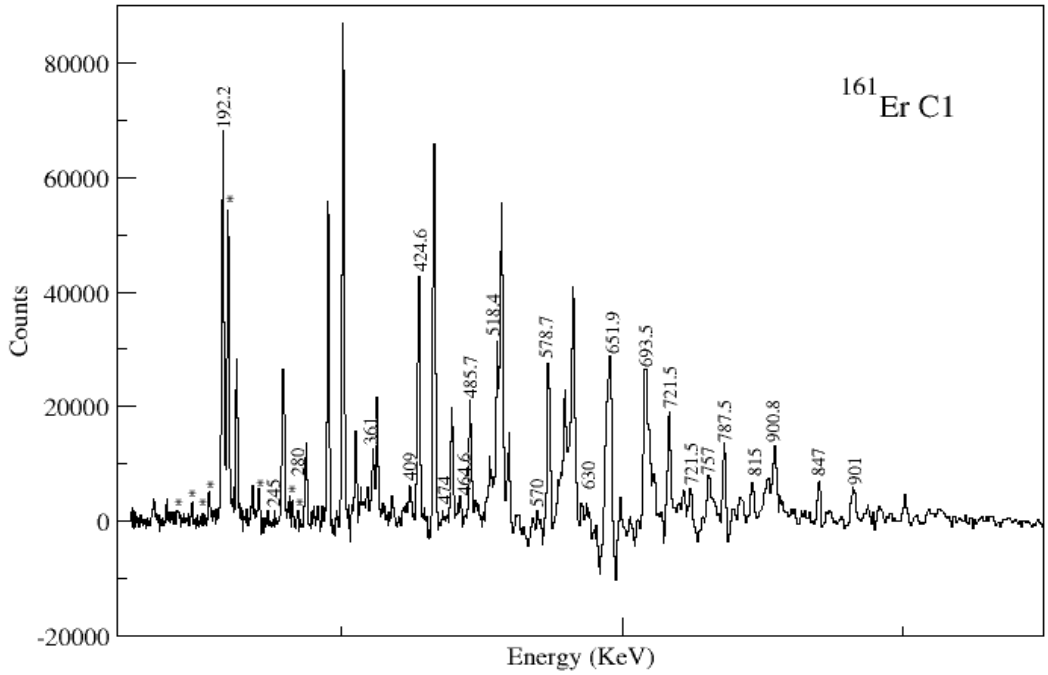

Figure 5. γ-ray coincidence spectrum for the C1 band in ^{161}Er

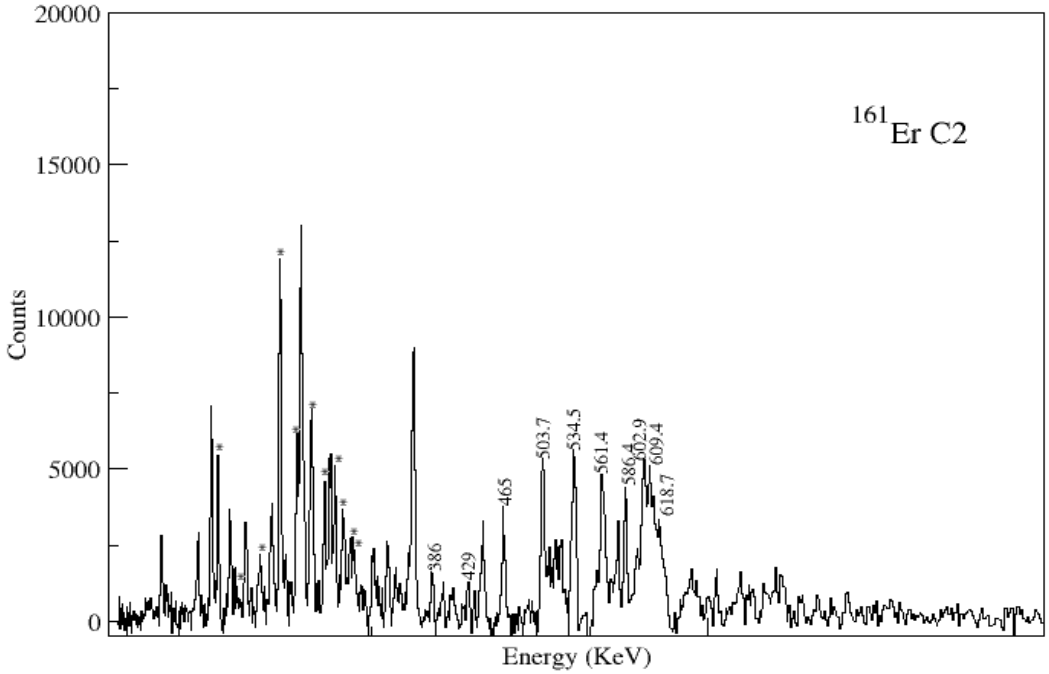

Figure 6. γ-ray coincidence spectrum for the C2 band in ^{161}Er

4.2 Alignments and band crossings in ^{161}Er

The peculiar The nucleus ^{161}Er is located in the well-prolate deformed region, has a characteristic revolving feature, and has Z = 68 and N = 93. To explore the effects of rotation on independent-particle motion in a deformed potential in ^{161}Er and to describe the properties of rotational bands at high spin, the experimental excitation energy and spins must be transformed to the rotating frame. For the yrast band and tightly linked bands seen in ^{161}Er nuclei, Figure 7 shows the typical plot of the aligned angular momentum (i) as a function of rotational frequency. The quasiparticle-aligned angular momentum is produced by deducting the reference angular momentum, $\omega J_0 + \omega^3 J_1$, from the total angular momentum along the rotating axis. The Harris parameters $J_0 = 27.8$ MeV^{-1} and J1 = 45.0 MeV^{-3} are used.

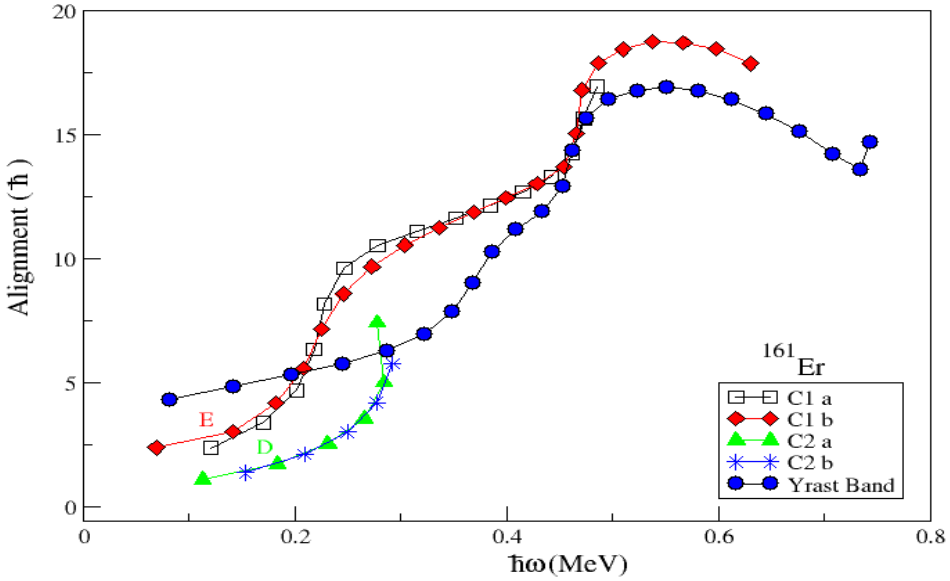

Figure 7. Experimental alignment versus rotational frequency of the strongly–coupled bands C1 and C2 compared with the yrast sequence in ^{161}Er nuclei. The Harris reference parameters are chosen to be J_0 =27.8.0MeV^{-1} and J_1 =45.0MeV^{-3}

The effect of multiple quasineutron alignments on strongly-coupled band structures is evident in the alignment behaviour of ^{161}Er [26]. The yrast band exhibits rather wide starting alignments of 4.33$\hbar$, and they undergo a noticeable up bend at $\hbar\omega\approx$0.37 MeV. The band crossing could be understood as the alignment of the neutrons BC [28, 29] . The second crossing yrast band at $\hbar\omega\approx$0.47 MeV corresponds to the $\pi h_{11/2}$ (ApBp) alignment, giving an additional gain of about 4.3$\hbar$. The proton alignment follows the neutron crossing by a slight amount. The two signature partners in the strongly coupled band C1 display comparable behaviour, and the initial band crossing takes place at $\hbar\omega\approx$ 0.23 MeV. The two signature partners display an alignment gain of roughly 6.5$\hbar$ following the band crossing, which is in line with the neutron AB alignment [23, 30, 31]. The alignment curves for the two signature partners bands are displayed in Figure 7. In the second band crossing in the strongly coupled band C1, corresponding to the $h_{11/2}$ (ApBp) proton alignment, takes place at $\hbar\omega\approx$0.47 MeV with an alignment gain of $\approx$ 6$\hbar$, indicating a significant nature inversion following the first band crossover in band C1. The configurations of bands C1 and C2 in ^{161}Er are identified for the first time. The two signature partners in the strongly coupled band C2 are nearly identical and exhibit the highest state seen. Band crossing occurs near the top of the strongly coupled band C2 with rotational frequency $\hbar\omega\approx$0.275 MeV. Since the crossing is not yet finished at the final transition shown, the alignment gain could not be determined in the current study. The band-crossing frequency is attributed to the neutron AB alignment since it is roughly equal to the yrast band in ^{162}Er [23, 31, 32]. The quasiparticle configurations, with rotational frequency at band crossings and alignment, of the strongly coupled bands of ^{161}Er are presented in Table 4 [23, 29]. Quasiparticle labelling for Nilsson quantum numbers at $\hbar\omega$ = 0 is explained in Table 5 [33] [22, 34, 35].

Table 4. Explains the quasiparticle configurations, with rotational frequency at band crossing (proton, neutron) in strongly coupled bands, in ^{161}Er [23, 29].

Band	Neutron	Alignment(i)	Proton	Alignment(i)	Configuration
^{161}Er – C1	0.23	6.5	0.47	6	E(F) →E(F)AB →E(F)ABE_pF_p
^{161}Er – C1	0.275	-			X(Y) →X(Y)AB

Table 5. Quasiparticle labelling scheme π = parity and α = signature [33, 35] .

	Label	$(\pi, \alpha)_n$	Nilsson quantum numbers
Quasineutrons	A	$(+, +1/2)_1$	$i_{13/2}$ [651] 3/2
	B	$(+, -1/2)_1$	$i_{13/2}$ [651] 3/2
	C	$(+, +1/2)_2$	$i_{13/2}$ [660] 1/2
	D	$(+, -1/2)_2$	$i_{13/2}$ [660] 1/2
	E	$(-, +1/2)_1$	$h_{9/2}$ [521] 3/2
	F	$(-, -1/2)_1$	$h_{9/2}$ [521] 3/2
	G	(−, +1/2)	*f* 7/2 [523] 5/2
	H	(−, -1/2)	*f* 7/2 [523] 5/2
	X	$(-, +1/2)_2$	$h_{11/2}$ [505] 11/2
	Y	$(-, -1/2)_2$	$h_{11/2}$ [505] 11/2
Quasiprotons	A_p	$(-, -1/2)_1$	$h_{11/2}$ [523] 7/2
	B_p	$(-, +1/2)_1$	$h_{11/2}$ [523] 7/2
	E_p	$(+, -1/2)_1$	$g_{7/2}$ [404] 7/2
	F_{pp}	$(+, +1/2)_1$	$g_{7/2}$ [404] 7/2

4.3 Calculation Parameters

An estimate of single-particle g-factors can be obtained using the relation:

$$g_k = g_l \pm \frac{l}{2l+1}\{g_s - g_l\}, \qquad (8)$$

where l+1/2 orbitals have a plus sign and l-1/2 orbitals have a minus sign. The total single-particle g-factor (g_k) combines the orbital and spin contributions of a nucleon. For protons, the orbital g-factor (g_l) = 1, while for neutrons (g_l) = 0; the spin g-factor (g_s) = +5.586 for protons and (g_s) = −3.826 for neutrons.

These values, used in the Schmidt model, allow the evaluation of the magnetic moments of nucleons in specific orbitals. The resulting g-factors are listed in [14, 36, 37]. Proton g-factors are always positive, whereas neutron g-factors can be positive or negative depending on the $l \pm s$ coupling.

For rotational nuclei, g-factors are taken from cranking model calculations[16]. In calculating BM1/BE2 ratios, the single-particle g-factors (g1, g2, g3) are assigned to the quasiparticles forming each configuration (e.g., A, B, C or Ap, Bp) [14, 36, 37].

To extract the single-quasiparticle alignments used in our B(M1) and B(E2) estimates, we evaluate the experimental aligned angular momentum *i* from the gain in alignment; each alignment depends on the single-quasiparticle configuration and band-crossing configuration, such as AB and BC.

$$\Delta i_x = [i_x(\omega)]_{after} - [i_x(\omega)]_{before} \qquad (9)$$

measured at the crossing's beginning. In even-A nuclei, the ground-state (0-qp) band is the "before" value, whereas in odd-A nuclei, the yrast 1-qp band is the "before" value. This ensures that Δi_x indicates the alignment carried by the additional quasiparticle or particles AB for the initial $i_{13/2}$ Neutron pair, Ap, and BC for the second pair, respectively, Bp. Regarding the $h_{11/2}$, two protons. The number of band quantum numbers is [38].

Table 6. Parameters adopted for the calculation of B(M1)/B(E2) ratios in strongly coupled bands of ^{161}Er.

Band	$g_{\Omega 1}$	$g_{\Omega 1}$	$g_{\Omega 1}$	i_1	i_2	i_3	k_1	k_2	k_3
^{161}Er - C1	1.34	-0.30	-0.3	1.3	1.9	6.87	$7/2^-$	0	$3/2^-$
^{161}Er - C2		-0.30	-0.2		-0.3	-0.2		0	$11/2^-$

Table 6 lists, for each band, the quasiparticle alignments i_1, i_2, and i_3 at successive crossings, along with the corresponding K components k_1, k_2, k_3 of the configuration. Using these inputs together with the single-particle g factors by using ref [16, 36, 37], g_R =Z/A, and Q_0. From the adopted deformation, Theoretical values obtained by using the bm1be2 code written in FORTRAN. The program returns B(M1) and B(E2) versus spin from the particle–rotor formulas using the specified i and K Quoted uncertainties reflect the propagated errors in *i* and Q_0.

5. Results

The experimental results of measured B(M1)/B(E2) ratios and theoretical calculations for the strongly coupled bands in ^{161}Er have been assigned in the current work for the first time. The experimental results, shown as data points in Figure 8, agree well with the theoretical calculations (solid lines) for both configurations. M1 transition strength in ^{161}Er is noticeably weaker compared with previous studies on the neighbouring odd-mass nuclei ^{157,159}Er (Ref.[16]). The behaviour suggests that the increasing neutron number strongly influences the M1 strength. Furthermore, the band configuration also appears to have a significant effect on the M1 transition strength. The numerical results are presented in Tables 7 and 8.

Table 7. Gamma-ray transition energies and B(M1)/B(E2) ratios for ^{161}Er C1.

Transition	E_γ (keV)	B(M1)/B(E2)	B(M1)/B(E2)
$29/2^- \rightarrow 27/2^-$	292	0.251	0.05151
$27/2^- \rightarrow 25/2^-$	183	0.008	0.01901
$25/2^- \rightarrow 23/2^-$	276	0.0645	0.00204
$23/2^- \rightarrow 21/2^-$	177	0.127	0.00280
$21/2^- \rightarrow 19/2^-$	244	0.0324	0.02540
$19/2^- \rightarrow 17/2^-$	164	0.253	0.07848
$17/2^- \rightarrow 15/2^-$	196	0.8195	0.18308
$15/2^- \rightarrow 13/2^-$	140	0.014	0.40573
$13/2^- \rightarrow 11/2^-$	140	1.207	1.10200

Table 8. Gamma-ray transition energies and B(M1)/B(E2) ratios for ^{161}Er C2.

Transition	E_γ (keV)	B(M1)/B(E2)	B(M1)/B(E2)
$35/2^- \rightarrow 33/2^-$	270	2.147	2.69511
$33/2^- \rightarrow 31/2^-$	316	2.497	2.53414
$31/2^- \rightarrow 29/2^-$	306	1.815	2.38009
$29/2^- \rightarrow 27/2^-$	305	1.583	2.23335
$27/2^- \rightarrow 25/2^-$	298	1.444	2.09446
$25/2^- \rightarrow 23/2^-$	287	1.233	1.96425
$23/2^- \rightarrow 21/2^-$	275	2.103	1.84395
$21/2^- \rightarrow 19/2^-$	260	1.863	1.73558
$19/2^- \rightarrow 17/2^-$	243	2.392	1.64259
$17/2^- \rightarrow 15/2^-$	224	2.163	1.57146
$15/2^- \rightarrow 13/2^-$	204	1.151	1.53599
$13/2^- \rightarrow 11/2^-$	182	0.954	1.57150

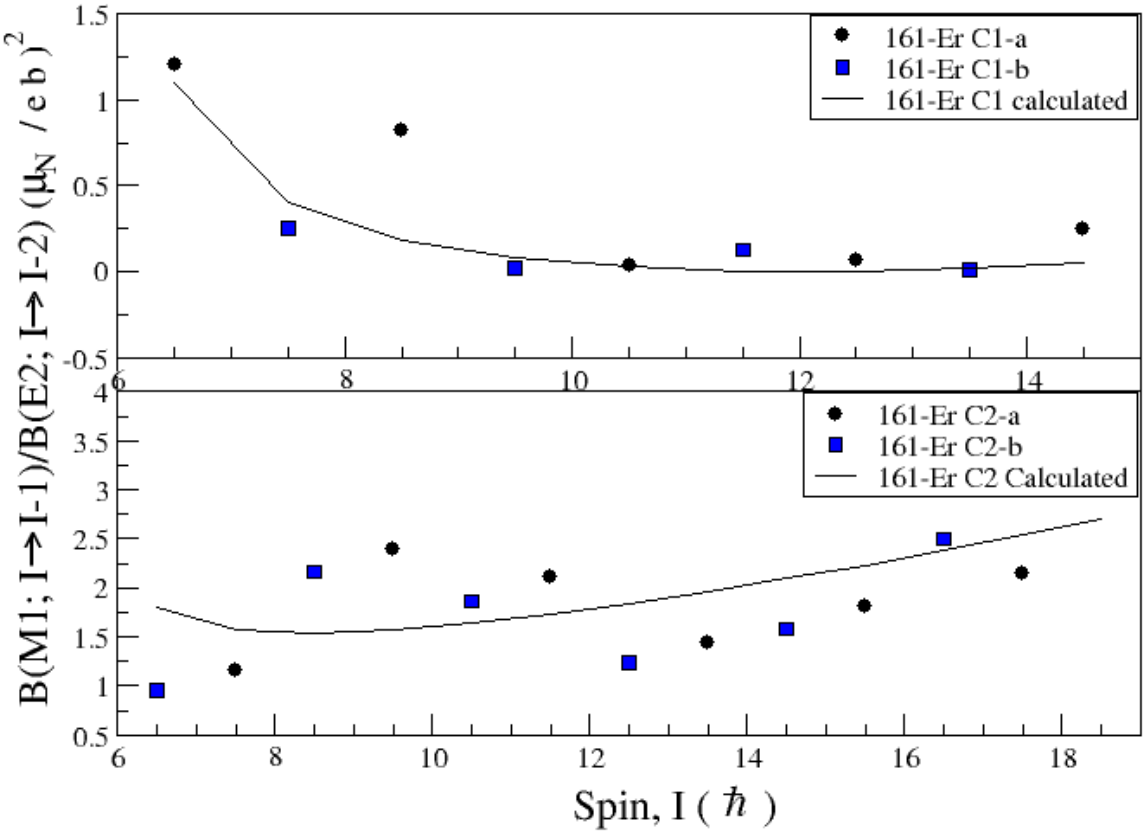

Figure 8. Experimental B(M1)/B(E2) ratios as a function of spin for ^{161}Er, compared with theoretical calculations for the proposed configurations.

6. Conclusion

The experiment was conducted at the ATLAS facility of Argonne National Laboratory, with data collected using the Gammashperearray and analysed using the RADWARE program. For the first time, the B(M1)/B(E2) ratios of the strongly coupled bands in ^{161}Er were measured. Based on the analysis, the configurations of the yrast and strongly coupled bands ^{161}Er were successfully assigned. The results indicate that the M1 transition strength decreases with increasing neutron number. These

findings provide a valuable foundation for future investigations aimed at identifying new transitions within strongly coupled bands and exploring additional rotational structures in ^{161}Er.

7. Acknowledgments:

I would like to express my sincere gratitude to Mr. Sarbast Rasull Mhamad, Research Center, University of Raparin, for his valuable assistance with the installation of the RADWARE program and for his guidance in learning its use. His support and encouragement were greatly appreciated throughout this work.

8. Declarations

The author declares that the results of this research were conducted independently as part of M.Sc. studies at the University of Koya. No funding was received for this work, and I declare no conflicts of interest.

8.1 Ethics Approval and Consent to Participate

Not applicable. This research did not involve human participants or animal subjects.

8.2 Consent for publication

Not applicable

8.3 Availability of Data and Materials

Data will be provided upon receiving a valid request.

8.4 Conflicts of interest

The authors declare that there is no conflict of interest

8.5 Funding

The authors state that none of their personal ties or known conflicting financial interests might have appeared to have influenced the work described in this study.

Authors' contributions

First Author.: Methodology, Writing - review & editing.

Second Author: Conceptualization, Data curation, Methodology, Writing - original draft.

9. References

[1] N. Bohr and J. A. Wheeler, "The mechanism of nuclear fission," *Physical Review,* vol. 56, no. 5, p. 426, 1939.

[2] A. Vinayak, M. Hosamani, P. Patil, and N. Badiger, "Determination of single neutron spectroscopic factor of doubly shell closed, neutron shell closed and neutron-rich nuclei through (d,p) reaction," *International Journal of Modern Physics E,* vol. 29, p. 2050030, 06/01 2020, doi: 10.1142/S0218301320500305.

[3] D. Radford, M. Cromaz, and C. Beyer, "Proceedings of the Nuclear Structure'98 Conference, Gatlinburg, 1998," ed: American Institute of Physics New York, 1999.

[4] M. G. Mayer, "On closed shells in nuclei. II," *Physical Review,* vol. 75, no. 12, p. 1969, 1949.

[5] J. D. Jensen, "Glimpses at the history of the nuclear structure theory," *The Nobel Prize in Physics,* 1963.

[6] C. Beausang *et al.*, "Using high-fold data from the new generation of γ-ray detector arrays," *Nuclear Instruments & Methods in Physics Research Section A-accelerators Spectrometers Detectors and Associated Equipment - NUCL INSTRUM METH PHYS RES A,* vol. 364, pp. 560-566, 10/01 1995, doi: 10.1016/0168-9002(95)00438-6.

[7] T. Bengtsson and I. J. N. P. A. Ragnarsson, "Rotational bands and particle-hole excitations at very high spin," vol. 436, no. 1, pp. 14-82, 1985.

[8] C. G. Andersson, J. Krumlinde, G. Leander, and Z. Szymański, "Rotational bands on few-particle excitations of very high spin," *Nuclear Physics A,* vol. 361, pp. 147-178, 05/01 1981, doi: 10.1016/0375-9474(81)90474-7.

[9] S. G. J. D. M. F. M. Nilsson, "Binding states of individual nucleons in strongly deformed nuclei," vol. 29, no. CERN-55-30, pp. 1-69, 1955.

[10] W. Nazarewicz, J. Dudek, R. Bengtsson, T. Bengtsson, and I. Ragnarsson, "Microscopic study of the high-spin behaviour in selected A ≃ 80 nuclei," *Nuclear Physics A,* vol. 435, pp. 397-447, 03/01 1985, doi: 10.1016/0375-9474(85)90471-3.

[11] I. Ragnarsson and S. Nilsson, "Shapes and Shells in Nuclear Structure," 09/01 2005.

[12] R. Bengtsson and S. Frauendorf, "Quasiparticle spectra near the yrast line," *Nuclear Physics A,* vol. 327, no. 1, pp. 139-171, 1979.

[13] S. M. Harris, "Higher order corrections to the cranking model," *Physical Review,* vol. 138, no. 3B, p. B509, 1965.

[14] A. O. Evans *et al.*, "High-Spin Structure beyond Band Termination in Er 157," *Physical review letters,* vol. 92, p. 252502, 07/01 2004, doi: 10.1103/PhysRevLett.92.252502.

[15] A. O. Evans, "Lifetime measurements in 112,110 Te and band termination and beyond in 157Er," University of Liverpool, 2004.

[16] A. O. Evans *et al.*, "High-spin structure in 157Er up to and above band termination," *Phys. Rev. C,* vol. 73, 06/15 2006, doi: 10.1103/PhysRevC.73.064303.

[17] J. Simpson *et al.*, "Discrete line γ-ray spectroscopy in the (50–60)ħ spin domain of 161,162Er," *Physical Review C,* vol. 62, 07/25 2000, doi: 10.1103/PhysRevC.62.024321.

[18] Y. Gono, D. Zolnowski, D. Heanni, and T. Sugihara, "Parity determination of high-spin yrast levels in 156Er," *Physics Letters B - PHYS LETT B,* vol. 49, pp. 338-340, 04/01 1974, doi: 10.1016/0370-2693(74)90175-0.

[19] J. Garrett *et al.*, "Evidence for Decreased Pairing Energies in Odd-N Nuclei from Band-Crossing Frequencies," *Physical Review Letters - PHYS REV LETT,* vol. 47, pp. 75-78, 07/01 1981, doi: 10.1103/PhysRevLett.47.75.

[20] M. Deleplanque *et al.*, "New structures at high spin in 159Er," *Physics Letters B,* vol. 193, no. 4, pp. 422-426, 1987.

[21] M. Riley, J. Garrett, J. Simpson, and J. Sharpey-Schafer, "Unpaired band crossings," *Physical Review Letters,* vol. 60, no. 7, p. 553, 1988.

[22] M. Mustafa *et al.*, "Diverse collective excitations in 159Er up to high spin," *Phys. Rev. C,* vol. 84, 11/22 2011, doi: 10.1103/PhysRevC.84.054320.

[23] L. Chen, X. Zhou, Y. Zhang, S. Zhang, and L. Zhu, "Properties of the 3/2−[521] band in the odd-N rare-earth nuclei," *Science China Physics, Mechanics and Astronomy,* vol. 54, no. Suppl 1, pp. 37-43, 2011.

[24] M. J. P. R. C.-N. P. Petri, "Evolution of structure and shapes in 158Er to ultrahigh spin," 2023.

[25] L. Chen *et al.*, "Reinvestigation of the high spin states in 161Er and enhanced E1 transitions in the N= 93 isotones," vol. 35, no. 6, p. 545, 2011.

[26] S. Wang, "Reinvestigation of the high spin states in 161Er and enhanced E1 transitions in the N = 93 isotones," *Chinese Physics C,* vol. 35, p. 545, 06/09 2011, doi: 10.1088/1674-1137/35/6/007.

[27] L. Chen *et al.*, "Properties of the rotational bands in^{161} Er," *Physical Review C,* vol. 83, p. 033418, 05/19 2013, doi: 10.1103/PhysRevC.83.034318.

[28] J. Simpson *et al.*, "Rotational alignment in 158Er and 159Er," *Journal of Physics G: Nuclear Physics,* vol. 10, p. 383, 01/01 1999, doi: 10.1088/0305-4616/10/3/012.

[29] G. B. Hagemann *et al.*, "Interactions between a multitude of rotational bands in well deformed odd nuclei: A new method for spin and parity assignment," *Nuclear Physics A,* vol. 618, pp. 199-237, 05/01 1997, doi: 10.1016/S0375-9474(97)00056-0.

[30] J. Simpson *et al.*, "Near-yrast discrete line γ-ray spectroscopy of 159Er and 160Er to I≳40*ħ*," *Journal of Physics G: Nuclear Physics,* vol. 13, p. 847, 01/01 1999, doi: 10.1088/0305-4616/13/6/013.

[31] H. Ryde, "High angular momentum phenomena workshop in honour of zdzisŁaw szymański," vol. 27, pp. 15-19, 01/01 1996.

[32] J. D. Garrett *et al.*, "Configuration dependent pairing from band crossing frequencies," *Physics Letters B,* vol. 118, pp. 297-302, 12/01 1982, doi: 10.1016/0370-2693(82)90188-5.

[33] J. Simpson *et al.*, "High-K quasiparticle structures in 159Er and 160Er," *European Physical Journal A,* vol. 1, pp. 267-274, 01/03 1998, doi: 10.1007/s100500050061.

[34] J. Simpson *et al.*, "Evolution of structure and shapes in Er 158 to ultrahigh spin," *Physical Review C,* vol. 107, 05/10 2023, doi: 10.1103/PhysRevC.107.054305.

[35] J. Ollier *et al.*, "Structure changes in ^{160}Er from low to ultrahigh spin," *Phys.Rev. C,* vol. 83, p. 044309, 04/12 2011, doi: 10.1103/PhysRevC.83.044309.

[36] A. Bohr and B. R. Mottelson, *NUCLEAR STRUCTURE. VOLUME I. SINGLE-PARTICLE MOTION*. 1969.

[37] D. Blaschke, H. Horiuchi, P. Ring, and G. Röpke, "The nuclear many-body problem," *The European Physical Journal A,* vol. 60, pp. 1-4, 09/01 2024, doi: 10.1140/epja/s10050-024-01384-6.

[38] S. Frauendorf, "Spontaneous symmetry breaking in rotating nuclei," *Reviews of Modern Physics - REV MOD PHYS,* vol. 73, pp. 463-514, 06/01 2001, doi: 10.1103/RevModPhys.73.463.

قياس الانتقال الكهرومغناطيسي المختزل (BM1/BE2) في النطاقات المقترنة بقوة في نوى 161Er

جوتيار لقمان مولان[1*] ، محمد إبراهيم محمد[2]

[1] قسم الفيزياء، كلية العلوم والصحة، جامعة كوية، كوية 44023، إقليم كردستان – العراق
[2] قسم الفيزياء، كلية العلوم، جامعة رابرين، رانية، السليمانية، 46012، العراق

المستخلص:

تقدم هذه الدراسة أول فحص لنسب احتمالات الانتقال الكهرومغناطيسي المخفضة للنطاقات المقترنة في نوى الإربيوم-161، والتي يتم إنتاجها من خلال تفاعلات الاندماج والتبخر باستخدام التفاعل 116 Cd (48Ca, 3γ)عند طاقة شعاع تبلغ MeV215 ، وذلك باستخدام مطياف كاماسفير (Gammashpere). تم تحليل النسب التجريبية لـ B(M1)/B(E2) من طيف التزامن باستخدام برنامج Radware ومقارنتها بالحسابات النظرية لدراسة تطور شدة انتقالات ثنائي القطب المغناطيسي ورباعي القطب الكهربائي عبر النطاقات المقترنة. تتوافق نسب B(M1)/B(E2) مع الاتجاهات المنهجية في النظائر المجاورة؛ ومع ذلك، فإنها تُظهر انخفاضًا في شدةM1 ، خاصةً عند البرم المنخفض مع زيادة عدد النيوكليونات. يشير هذا الانخفاض إلى انخفاض في مركبة ثنائي القطب المغناطيسي المرتبطة بالتغيرات في التكوين شبه الجسيم الأساسي (quasiparticle). تتطابق النتائج التجريبية بشكل وثيق مع الحسابات النظرية، مما يؤكد صحة التكوينات المقترحة ويوسع نطاق منهجية نسب B(M1)/B(E2) ضمن سلسلة نظائر الإربيوم.